**International Journal of Power Electronics and Drive System (IJPEDS)**
Vol. 17, No. 1, March 2026, pp. 809~822
ISSN: 2088-8694, DOI: 10.11591/ijpeds.v17.i1.pp809-822 

# Design and implementation of a buck converter–based PV emulator using dynamic evolution control

**Ahmad Saudi Samosir, Dikpride Despa, Herri Gusmedi, Sony Ferbangkara**
Department of Electrical Engineering, Faculty of Engineering, Universitas Lampung, Bandar Lampung, Indonesia

**Article Info**

***Article history:***

Received Nov 22, 2025
Revised Feb 10, 2026
Accepted Feb 21, 2026

***Keywords:***

Buck converter
Dynamic evolution control
MATLAB/Simulink
MPPT
PV emulator

**ABSTRACT**

This paper presents the design, simulation, and experimental implementation of a photovoltaic (PV) emulator based on a buck converter controlled using the dynamic evolution control (DEC) technique. The proposed system accurately reproduces the nonlinear current-voltage (I-V) and power-voltage (P–V) characteristics of a commercial GREEN CELL SM100-18P (100 Wp) PV module under standard test conditions (1000 W/m$^2$, 25 °C). The electrical characteristics of the reference module are embedded in the controller through a lookup table (LUT), which is integrated with the DEC algorithm to enable adaptive real-time regulation of output voltage and current. System modeling and validation are first conducted in MATLAB/Simulink to analyze steady-state and transient performance. A hardware prototype based on an XL4016 buck converter and Arduino Nano microcontroller is then implemented, with real-time monitoring provided via an ILI9341 TFT display. Experimental results show that the emulator achieves a maximum power deviation of 0.8%, a normalized root mean square error (RMSE) of 0.015, a settling time of approximately 12 ms, overshoot below 1.5%, voltage ripple under 2%, and peak conversion efficiency of 94% near the MPP region. These results confirm that the proposed PV emulator provides accurate static and dynamic reproduction of PV characteristics, offering a low-cost, stable, and repeatable platform for laboratory-scale evaluation of PV-related power electronic converters.



***Corresponding Author:***

Ahmad Saudi Samosir
Department of Electrical Engineering, Faculty of Engineering, Universitas Lampung
Sumantri Brojonegoro St., No. 1, Bandar Lampung, Lampung 35145, Indonesia
Email: ahmad.saudi@eng.unila.ac.id, saudi.ahmad@gmail.com

## 1. INTRODUCTION

The rapid expansion of photovoltaic (PV) technology has played a central role in the global transition toward sustainable and renewable energy systems. Improvements in PV module design, manufacturing, and efficiency continue to drive widespread adoption across residential, commercial, industrial, and utility-scale applications [1]. As PV integration increases, accurate characterization and testing of PV-powered systems, particularly power converters and control strategies operating under PV conditions, become increasingly critical. However, direct testing using real PV modules is limited by their strong dependence on environmental conditions such as irradiance and temperature, which reduces reproducibility and makes controlled laboratory testing difficult. Consequently, PV emulators have emerged as an essential tool for indoor testing, enabling the reproduction of PV electrical characteristics under precisely controlled conditions [2], [3].

Recent research has demonstrated a variety of PV emulator architectures, ranging from programmable power supplies and electronic loads to converter-based designs [4]–[6]. Among these, DC–DC buck-converter-based emulators have gained significant interest due to their high efficiency, fast dynamic

response, compact implementation, and suitability for low-to-medium-power PV applications [7], [8]. Several studies have explored enhancements to emulator models, including partial-shading behavior [9], adaptive feedback controls [10], explicit PV-model-based emulation [11], FPGA-based real-time implementations [12], and fast-dynamic control strategies [13]–[16]. Despite these advances, PV emulator research remains relatively limited when compared to broader PV system studies, and low-cost solutions suitable for laboratory environments are still in high demand.

Several recent studies have further advanced PV emulator performance through improved modeling and control strategies. Harrison and Alombah [17] developed a high-performance PV emulator capable of accurately reproducing PV characteristics under dynamic operating conditions, which is a fundamental requirement for MPPT controller evaluation. In a subsequent work, the same authors introduced a piecewise-segmentation-based PV emulator using artificial neural networks combined with a nonlinear backstepping controller, achieving enhanced tracking accuracy and dynamic behavior [18]. Henry et al. [19] proposed an explicit PV-model-based emulator that significantly reduces computational burden while maintaining fast response and high fidelity. Moreover, Harrison *et al.* [20] presented an enhanced control strategy based on shift methodology, enabling reliable PV emulation under continuously changing environmental conditions.

Despite these advances, many reported solutions rely on complex hardware platforms, high-performance digital controllers, or computationally intensive algorithms [17]–[21]. As a result, affordable microcontroller-based PV emulators suitable for academic laboratories remain limited. Furthermore, low-cost implementations commonly employ proportional–integral–derivative (PID) controllers [22]–[24], which require extensive gain tuning and may exhibit degraded tracking performance when reproducing highly nonlinear current–voltage (I–V) and P–V characteristics, particularly near the maximum power point (MPP). Overshoot, oscillation, and slow convergence may be observed under dynamic load variations.

To overcome these limitations, dynamic evolution control (DEC) has emerged as an attractive nonlinear control approach for power electronic systems. DEC enforces error convergence along predefined exponential trajectories, yielding smooth and monotonic transient responses with minimal tuning effort [25]–[28]. While DEC has demonstrated robustness in DC–DC converter regulation, its application to PV emulator control remains largely unexplored in the literature. In parallel, significant progress has been made in PV modeling, including single-diode models, multi-parameter formulations, and machine-learning-based approaches [29]–[32]. Accurate incorporation of irradiance and temperature effects under standard test conditions (STC) is essential for reliable emulator performance [33]–[35]. Nevertheless, commercial PV emulators remain costly and often inaccessible for small research groups and educational institutions [5], [17].

These observations reveal a clear research gap: the absence of a low-cost, microcontroller-based PV emulator that integrates accurate nonlinear PV modeling with a modern nonlinear control strategy while maintaining real-time performance and implementation simplicity. To address this gap, this paper proposes a buck-converter-based PV emulator regulated by DEC. The GREEN CELL SM100-18P (100 Wp) PV module is selected as the reference source under standard test conditions (1000 W/m², 25 °C). Its electrical characteristics are embedded into the controller via a lookup table (LUT) derived from MATLAB/Simulink modeling, enabling real-time reproduction of nonlinear I–V and P–V curves with low computational overhead on an Arduino Nano platform.

The main contributions of this work are threefold: i) A low-cost PV emulator architecture integrating DEC with LUT-based nonlinear PV modeling, avoiding the complexity of neural or adaptive controllers; ii) Experimental implementation of DEC on a resource-constrained microcontroller for real-time buck converter regulation; and iii) Comprehensive simulation and experimental validation demonstrating accurate PV characteristic reproduction and competitive dynamic performance under load variations. It is emphasized that the primary objective of this study is accurate PV characteristic emulation. Although the proposed platform is suitable for future MPPT investigations, MPPT implementation and evaluation are beyond the scope of this work.

## 2. METHOD

### 2.1. Proposed buck converter–based PV emulator

The proposed system is designed to emulate the nonlinear I–V and power–voltage (P–V) characteristics of a PV module under STC. In this study, the GREEN CELL SM100-18P (100 Wp) crystalline silicon photovoltaic module is explicitly selected as the reference PV source for emulator development. The key electrical parameters of this module under STC are specified and summarized in a dedicated parameter table, which serves as the reference for generating the target I–V and P–V characteristics.

The emulator integrates a photovoltaic reference model stored in a LUT with a DEC algorithm executed on an Arduino Nano microcontroller. A synchronous buck converter based on the XL4016 power

module functions as the power stage responsible for reproducing the nonlinear electrical output of the reference PV module. Real-time monitoring and visualization are provided through an ILI9341-based TFT display, enabling the system to operate as an interactive platform for observing PV behavior and validating emulation performance under varying load conditions.

The proposed PV emulator is composed of three main subsystems: i) Power stage: a buck converter that regulates the output voltage and current in accordance with the pulse width modulation (PWM) control signal generated by the microcontroller; ii) Control stage: an Arduino Nano that acquires real-time voltage and current measurements, retrieves the corresponding reference values from the LUT, computes the control error, and updates the switching duty cycle using the DEC algorithm; and iii) Monitoring and display stage: an ILI9341-based TFT module that provides real-time visualization of the output voltage, output current, output power, reconstructed I–V characteristics, and the instantaneous operating point.

Figure 1 illustrates the overall system architecture of the proposed buck-converter-based PV emulator. The system is powered by a regulated 24 V DC supply, while the controller continuously executes the DEC control loop to ensure that the converter output accurately tracks the target photovoltaic characteristics derived from the reference PV model. The formulation of this reference PV model, along with the generation of the corresponding LUT based on the selected PV module parameters under STC, is described in detail in Section 2.2.

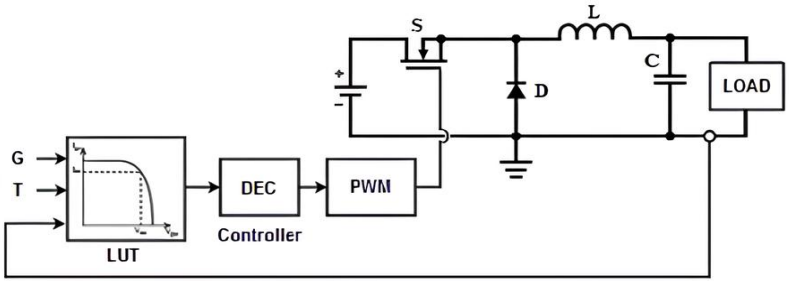


Figure 1. Main circuit of the proposed buck converter–based PV emulator

### 2.2. Development of the PV model operating points and LUT generation

In this study, the GREEN CELL SM100-18P photovoltaic module, rated at 100 Wp, is selected as the reference PV source for emulator development. The electrical specifications of this module under STC, defined as an irradiance of 1000 W/m² and a cell temperature of 25 °C are summarized in Table 1 and serve as the basis for PV model generation and emulator reference construction.

To accurately determine the nonlinear, I–V and P–V operating characteristics of the reference PV module, a complete PV model was developed in MATLAB/Simulink, as illustrated in Figure 2. The simulation was conducted under STC conditions to ensure consistency with the manufacturer's datasheet. A set of resistive load variations was applied to the PV model to extract operating points across the entire electrical operating range.

By varying the load resistance from low to high values, the simulation captured the full I–V characteristic, spanning from the short-circuit current (Isc) region to the open-circuit voltage (Voc) region. For each load condition, the corresponding voltage, current, and output power were recorded, providing a comprehensive set of PV operating points.

The resulting dataset was sampled and discretized to construct a LUT, which is embedded in the memory of the Arduino Nano microcontroller. During real-time operation, the measured emulator output voltage is used as the LUT index to retrieve the corresponding reference current and power values. Linear interpolation between adjacent LUT points is applied to ensure smooth transitions and accurate tracking performance during rapid load variations.

Table 1. Electrical specifications of the Green Cell SM100-18P module under STC

| Parameter | Symbol | Value | Unit |
|---|---|---|---|
| Maximum power | Pmax | 100 | W |
| Voltage at MPP | Vmp | 17.8 | V |
| Current at MPP | Imp | 5.62 | A |
| Open-circuit voltage | Voc | 21.8 | V |
| Short-circuit current | Isc | 6.05 | A |

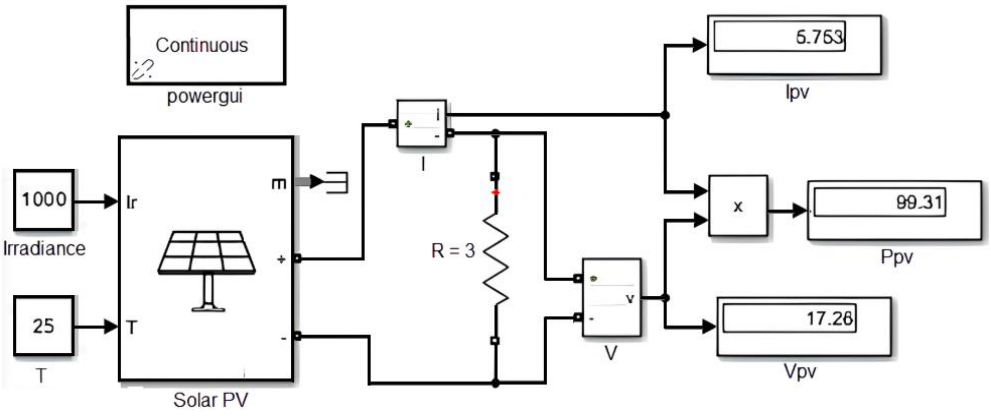


Figure 2. MATLAB/Simulink model captured the I–V characteristic of GREEN CELL SM100-18P

This LUT-based modeling approach enables faithful reproduction of the nonlinear electrical characteristics of the GREEN CELL SM100-18P PV module while maintaining low computational complexity, making it well suited for real-time implementation on a resource-limited microcontroller platform. By relying on precomputed PV operating points rather than online parameter estimation, the proposed LUT structure also reduces sensitivity to parameter uncertainties and measurement noise, thereby enhancing the robustness of the overall emulation system when combined with the DEC strategy.

### 2.3. Design of the buck converter

The power conversion stage of the emulator employs a buck converter topology due to its high efficiency and suitability for reproducing the nonlinear behavior of a PV module. The converter is implemented using the XL4016 module, which integrates the MOSFET switch, gate driver, and protection circuitry. The Arduino Nano generates a 31.25 kHz PWM signal to control the MOSFET gate. By adjusting the duty cycle according to the DEC algorithm, the converter output dynamically follows the I–V curve of the reference PV model stored in the LUT.

The inductance and capacitance values were determined based on standard continuous conduction mode (CCM) design equations. The inductor value is calculated as (1).

$$L = \frac{(V_{in} - V_{out}).D}{f_S.\Delta I_L} \quad (1)$$

Where $f_S$ is the switching frequency and $\Delta I_L$ is the allowable inductor ripple current. The output capacitor is determined as (2).

$$C = \frac{\Delta I_L}{8 f_S.\Delta V_{out}} \quad (2)$$

Where $\Delta V_{out}$ represents the acceptable output voltage ripple.

Based on these design equations, a 470 µH inductor is selected to maintain continuous conduction mode while keeping the current ripple below 20%. A 470 µF low-ESR output capacitor is employed to ensure stable voltage with minimal ripple. The switching frequency is set to 31.25 kHz, corresponding to the highest PWM resolution supported by the Arduino Nano. The load resistance range is defined between 0.5–100 Ω to represent variable resistive or electronic loads during emulator testing.

These parameter selections ensure stable CCM operation, low output ripple, and adequate dynamic response under rated conditions. Figure 3 presents the schematic diagram of the proposed buck-converter-based PV emulator, and the complete design parameters are summarized in Table 2.

### 2.4. Design of the dynamic evolution control algorithm

Dynamic evolution control (DEC) is employed in this study due to its strong capability in handling nonlinear systems with minimal tuning requirements. The fundamental principle of DEC is to regulate the system error dynamics by explicitly constraining them to follow a predefined evolution path. By enforcing this constraint, the tracking error is guaranteed to decrease smoothly and monotonically from its initial value toward zero, ensuring stable and predictable convergence.

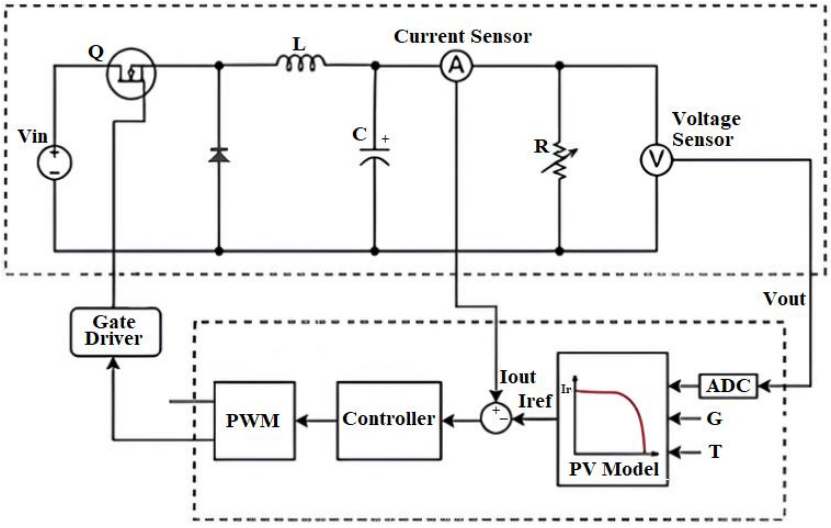


Figure 3. Schematic diagram of the buck converter-based PV emulator system

Table 2. Load data of the PV emulator with varying resistors

| Load resistance (Ω) | PV voltage (V) | PV current (A) | PV power (W) |
|---|---|---|---|
| 100 | 21.71 | 0.2171 | 4.715 |
| 50 | 21.63 | 0.4326 | 9.357 |
| 25 | 21.46 | 0.8583 | 18.42 |
| 15 | 21.22 | 1.415 | 30.03 |
| 10 | 20.92 | 2.092 | 43.76 |
| 8 | 20.68 | 2.585 | 53.45 |
| 5 | 19.87 | 3.973 | 78.94 |
| 4 | 19.16 | 4.79 | 91.77 |
| 3 | 17.26 | 5.753 | 99.31 |
| 2 | 11.93 | 5.946 | 71.14 |
| 1 | 6.007 | 6.007 | 36.08 |
| 0.5 | 3.014 | 6.028 | 18.17 |
| 0.2 | 1.208 | 6.041 | 7.3 |

The predefined evolution path, referred to as the dynamic evolution trajectory, is commonly modelled using an exponential decay function. Let Y(t) denote the dynamic evolution variable associated with the system error. Its evolution is defined as (3).

$$Y(t) = Y_o . e^{-mt} \quad (3)$$

Where $Y_O$ is the initial value of the dynamic variable, and (m > 0) is the evolution rate parameter that determines the convergence speed. Differentiating (1) with respect to time yields the dynamic evolution function [23].

$$\frac{dY(t)}{dt} + mY(t) = 0 \quad (4)$$

Which enforces a strictly decreasing error trajectory toward zero.

To apply DEC to the voltage regulation problem of the PV emulator, the dynamic variable is defined based on the output voltage tracking error as (5).

$$Y = k.V_{err} = k(V_{ref} - V_o) \quad (5)$$

Where $V_{ref}$ is the reference voltage obtained from the LUT, $V_o$ is the measured output voltage, and k>0 is a scaling coefficient that adjusts the sensitivity of the evolution dynamics.

Substituting (5) and its derivative into (4) yields:

$$k\frac{dV_{err}}{dt} + m.k.V_{err} = 0 \quad (6)$$

For the buck converter operating in continuous conduction mode (CCM), the output voltage dynamics can be approximated by the averaged steady-state relationship.

$$V_o = D.V_{in} - L\frac{diL}{dt} \quad (7)$$

Where D is the PWM duty cycle, and Vin is the input voltage. Summing the converter operating point (7) into (6), we can get:

$$k\frac{dV_{err}}{dt} + m.k.V_{err} + V_o = D.V_{in} - L\frac{diL}{dt}$$

Solving for the control input D, the DEC-based duty-cycle equation is given by [28] as (8).

$$D = \frac{k.\frac{dV_{err}}{dt} + m.k.V_{err} + V_o + L\frac{diL}{dt}}{V_{in}} \quad (8)$$

The (8) represents the DEC-based duty-cycle law that directly links the converter control input to the voltage tracking error and its prescribed evolution dynamics.

By enforcing this control law, the voltage tracking error is constrained to follow the exponential evolution path defined in (3), guaranteeing monotonic convergence of the output voltage $V_O$ toward the reference voltage $V_{ref}$ with a convergence rate governed by the parameter m. In this study, the parameters k = 0.1 and m = 3000 were selected through experimental tuning to achieve fast convergence while avoiding overshoot and oscillatory behavior. At each sampling instant, the Arduino Nano measures the output voltage and current, retrieves the corresponding reference values from the LUT, computes the tracking error, and updates the PWM duty cycle according to (8).

### 2.5. Stability analysis of the dynamic evolution control

The stability of the proposed DEC scheme can be rigorously analyzed based on the prescribed error evolution dynamics. As defined in Section 2.4, the dynamic evolution variable is expressed as:

$$Y = k(V_{\text{ref}} - V_o)$$

where $k > 0$. The evolution constraint imposed by DEC enforces.

$$\dot{Y} = -mY, m > 0$$

To analyze stability, a Lyapunov candidate function is selected as:

$$V(Y) = \frac{1}{2}Y^2$$

which is positive definite for all $Y \neq 0$. Taking the time derivative of $V$ yields:

$$\dot{V} = Y\dot{Y}$$

substituting the evolution constraint gives:

$$\dot{V} = -mY^2$$

since $m > 0$, it follows that:

$$\dot{V} < 0 \; \forall \; Y \neq 0$$

which guarantees that the equilibrium point $Y = 0$, corresponding to $V_o = V_{\text{ref}}$, is globally asymptotically stable. Therefore, the DEC law ensures exponential convergence of the voltage tracking error to zero.

Furthermore, the convergence rate is explicitly governed by the parameter $m$, allowing a direct trade-off between response speed and control effort. This explicit stability property distinguishes DEC from conventional PI-based controllers, where stability margins depend strongly on tuning accuracy and operating conditions.

### 2.6. Hardware realization and system integration

The complete hardware realization integrates the buck converter power stage, sensing circuitry, digital controller, and visualization interface into a unified PV emulation platform. The power stage is implemented using an XL4016-based buck converter, while real-time voltage and current measurements are obtained through dedicated sensing circuits interfaced with the analog-to-digital converter (ADC) of the Arduino Nano.

To implement the developed emulator, several key electrical variables are measured using appropriate sensors. The emulator output voltage (Vo) is sensed through a resistive voltage divider connected to the Arduino Nano ADC, enabling measurement within a 0–30 V range and providing voltage feedback for the DEC regulation. The output current (Io) is measured using a Hall-effect current sensor (ACS712–20A) with a ±20 A measurement range, allowing accurate load current monitoring and real-time output power calculation.

In addition, the input voltage (Vin) of the buck converter is measured using a separate resistive voltage divider and ADC channel. This measurement is utilized for duty-cycle normalization, system monitoring, and over-voltage protection during emulator operation. The output power (Po) is not directly sensed but is computed in real time by the controller as the product of the measured output voltage and current (Po = Vo x Io). This computed power value is used to reconstruct the P–V characteristic curve and to validate the accuracy of the PV emulation.

The measured voltage and current signals are continuously sampled and processed by the digital controller to execute the DEC algorithm and update the PWM duty cycle in real time. This closed-loop operation enables accurate tracking of the reference voltage and current values derived from the LUT, ensuring faithful reproduction of the nonlinear I–V and P–V characteristics of the target PV module across a wide operating range. An ILI9341-based TFT display module is employed as a graphical user interface (GUI) to visualize key operating parameters, including output voltage, output current, and output power, as well as the reconstructed P–V characteristic curve and the instantaneous operating point. This visualization facilitates real-time observation of emulator behavior under varying load conditions and supports experimental validation of the control strategy.

All subsystems are powered from a regulated 24 V DC supply, providing sufficient headroom for emulating the selected 100 Wp PV module. The digital control loop operates synchronously with the configured PWM switching frequency, ensuring consistent sampling and stable control execution. To ensure reliable emulation fidelity, particular attention was given to sensor calibration and measurement accuracy. Prior to experimental testing, both the voltage divider and the Hall-effect current sensor were calibrated using a laboratory-grade digital multimeter to minimize offset and gain errors, with calibration factors applied in software.

Although low-cost sensors and a basic microcontroller are employed, the achieved measurement resolution is sufficient for accurate reproduction of the PV I–V and P–V characteristics under STC. Since the proposed DEC strategy relies on closed-loop feedback rather than absolute measurement precision at each sampling instant, small measurement uncertainties do not significantly affect overall emulation performance. This balance between measurement accuracy and implementation simplicity makes the proposed hardware platform well suited for laboratory-scale PV analysis and MPPT testing.

## 3. RESULTS AND DISCUSSION

### 3.1. Simulation results

The performance of the proposed buck converter-based PV emulator was comprehensively evaluated through extensive simulations conducted in MATLAB/Simulink. The overall simulation model consists of three main subsystems—the PV module, the buck converter power stage, and the DEC controller enhanced with a LUT. The overall model architecture is illustrated in Figure 4. Through this configuration, the dynamic characteristics of the PV emulator were examined to verify its capability to reproduce the I–V and P–V curves under STC, while also validating the transient response and stability of the DEC controller under varying load conditions and shifts in the operating point.

In this simulation, the PV characteristics were modelled based on the GREEN CELL SM100-18P module under STC, which correspond to an irradiance of 1000 W/m² and a cell temperature of 25 °C. The buck converter was simulated to operate with an input voltage (Vin) of 24 V, a switching frequency of 31.25 kHz, an inductance (L) of 0.5 mH, and a capacitance (C) of 440 µF.

The simulation results show that, in open circuit or no-load conditions, the PV emulator outputs a voltage of 21.8 V, the operating point is at the open circuit voltage (Voc), with a current of 0 A. When the solar panel module is loaded with a 10 Ω, the operating point shifts to Vo = 20.92 V and Io = 2.092 A, resulting in an output power of approximately 43.76 W. As the load resistance decreases, the output current increases, pushing the operating point toward the MPP region of approximately 100 W. If the load resistor is continuously reduced, the PV operating point will shift closer to the short-circuit point, namely at Vo ≈ 0 V and Io ≈ 6.05 A. Load data with varying resistors are shown in Table 2, which shows how different resistor values affect the electrical behavior of the PV emulator. This analysis confirms that the developed simulation model accurately reproduces the nonlinear behavior of real PV modules and provides a reliable foundation for validating the proposed DEC-based control strategy.

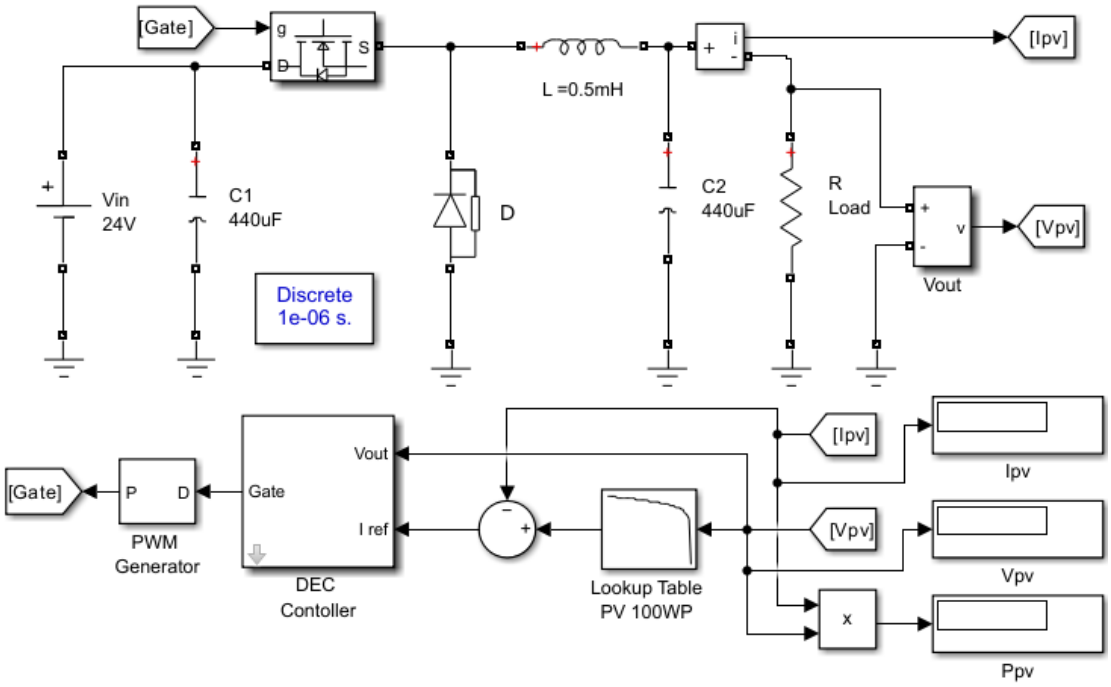


Figure 4. MATLAB Simulink model of buck converter-based PV emulator

### 3.1.1. Dynamic simulation under irradiance and load variations

To address realistic operating scenarios and to substantiate the experimental results, additional simulations were conducted under dynamic conditions involving abrupt changes in irradiance and load resistance. These tests are essential for evaluating the transient response, stability, and robustness of the proposed DEC-controlled PV emulator.

In the first scenario, step changes in irradiance were applied while maintaining a fixed load resistance. The irradiance was varied from 1000 W/m² to 600 W/m² and subsequently increased to 800 W/m², emulating rapidly changing environmental conditions. The simulation results show that the emulator output voltage and current smoothly transition to the new operating points without overshoot or oscillation. The power response converges rapidly toward the reference operating point corresponding to each irradiance level, demonstrating the strong dynamic tracking capability of the DEC algorithm.

In the second scenario, the load resistance was abruptly changed between high-resistance and low-resistance values to emulate sudden load disturbances. The DEC controller successfully maintains stable operation, forcing the emulator output to follow the reference I–V curve stored in the LUT. The transient response exhibits fast settling time and minimal ripple, indicating robust closed-loop performance.

These dynamic simulation results closely reflect the conditions encountered during experimental testing and confirm that the proposed emulator maintains accurate PV behavior not only in steady-state but also under rapidly changing operating conditions. The consistency between dynamic simulation and experimental observations provides strong validation of the proposed control strategy.

### 3.1.2. Comparison between LUT-based emulator and reference solar panel model

To further strengthen the validation, a direct comparison was performed between the LUT-based PV emulator and the analytical PV model of the GREEN CELL SM100-18P module. The I–V and P–V curves generated by the LUT were compared against the corresponding curves obtained from the mathematical PV model under identical STC conditions.

The comparison reveals a close agreement between the LUT-based emulator and the reference PV model across the entire operating range, including the open-circuit, MPP, and short-circuit regions. Minor deviations observed near the knee of the I–V curve are primarily attributed to discretization effects inherent to the LUT resolution and the finite precision of the microcontroller implementation. Nevertheless, these deviations remain within acceptable limits for laboratory-scale PV emulation and control algorithm testing. This comparison confirms that the LUT-based approach accurately represents the electrical behavior of the real PV module while offering a computationally efficient alternative suitable for low-cost microcontroller-based implementation.

### 3.2. Hardware implementation results

To validate the practical feasibility of the proposed PV emulator, a hardware prototype was developed using an XL4016-based buck converter controlled by an Arduino Nano microcontroller. The prototype was designed to reproduce the nonlinear current–voltage (I–V) and power–voltage (P–V) characteristics of a photovoltaic (PV) module under STC, corresponding to an irradiance level of 1000 W/m² and a temperature of 25°C. The overall hardware configuration of the buck-converter-based PV emulator is illustrated in Figure 5.

The DEC algorithm was implemented on the Arduino Nano to regulate the converter duty cycle in real time based on predefined reference characteristics. A lookup table (LUT) containing the I–V and P–V data of a commercial 100 Wp PV module, namely the GREEN CELL SM100-18P, was employed as the reference model. By continuously updating the duty cycle according to the DEC law, the emulator output voltage and current were forced to converge toward the LUT reference, enabling accurate emulation of PV behavior across a wide operating range.

To facilitate real-time monitoring and qualitative validation, an ILI9341 TFT display module was integrated as a GUI. The display provides real-time visualization of output voltage, current, and power, allowing direct observation of system behavior under different loading conditions. This interface also serves as a practical diagnostic tool for verifying controller performance during experimental testing.

The experimental evaluation was conducted by subjecting the emulator to various resistive loads in order to examine its steady-state and dynamic responses. Figures 6(a) and 6(b) present the TFT display readings when the emulator was connected to 20 Ω and 10 Ω resistive loads, respectively, representing moderate loading conditions near the maximum power point region. Figures 7(a) and 7(b) show the responses under heavier loading conditions of 2 Ω and 0.5 Ω, which push the emulator operation toward the high-current region of the I–V curve. In addition, Figure 8 illustrates the emulator behavior under no-load conditions, corresponding to the open-circuit voltage region of the PV characteristics.

Figure 5. Hardware prototype buck converter-based PV emulator

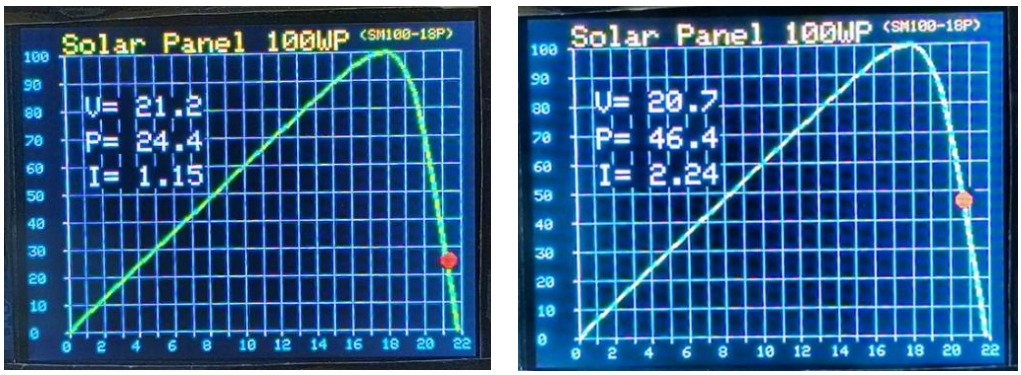


(a) (b)

Figure 6. TFT display during testing: (a) with 20-ohm load and (b) with 10-ohm load

The experimental results demonstrate that the emulator output closely follows the LUT-based reference characteristics of the Green Cell SM100-18P module across all tested conditions. The observed trends are consistent with the simulation results, particularly during load transitions, confirming that the DEC controller ensures stable, fast, and accurate tracking of the reference PV behavior. The strong agreement between dynamic simulations, LUT-based reference characteristics, and experimental measurements confirms that the proposed system provides a reliable and low-cost PV emulator suitable for laboratory validation of power converters and control algorithms operating under realistic PV conditions. A detailed quantitative evaluation of tracking accuracy, dynamic response, and converter efficiency is presented in section 3.3 to further substantiate the experimental validation.

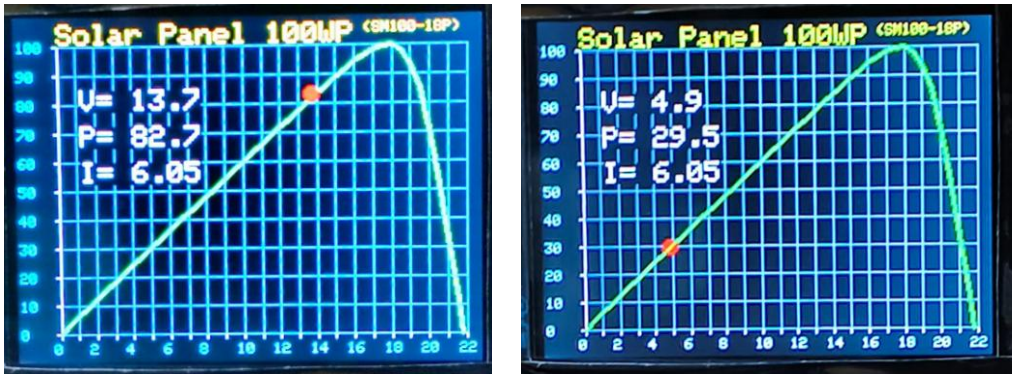


(a) (b)

Figure 7. TFT display during testing: (a) with 2-ohm load and (b) with 0.5-ohm load

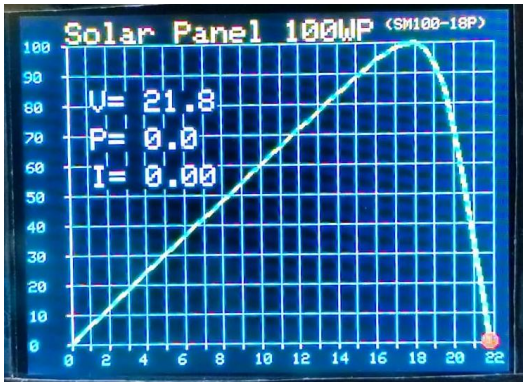


Figure 8. TFT display during no load testing

To provide a clearer quantitative validation of the experimental behavior, Table 3 summarizes the measured operating points of the proposed PV emulator under different resistive loads at STC conditions. The table lists the corresponding output voltage, current, and power for each load resistance, thereby representing discrete operating points along the emulated I–V curve. As shown in Table 3, the no-load condition yields an open-circuit voltage of 21.8 V, which closely matches the expected Voc of the reference module.

When the load resistance decreases from 20 Ω to 3 Ω, the output current increases progressively while the voltage gradually drops, consistent with the nonlinear PV characteristic. Notably, the maximum measured power of 99.2 W occurs at a load of 3 Ω, indicating operation near the maximum power point region of the reference module. For lower resistances (2 Ω and 0.5 Ω), the voltage drops significantly while the current approaches its saturation region (approximately 6 A), reflecting the short-circuit region behavior of a real PV module.

Table 3. Measured operating points of the proposed PV emulator under different resistive loads (STC conditions)

| Load resistance (Ω) | PV voltage (V) | PV current (A) | PV power (W) |
|---|---|---|---|
| No load | 21.8 | 0 | 0 |
| 20 | 21.2 | 1.15 | 24.4 |
| 10 | 20.7 | 2.24 | 20.7 |
| 5 | 19.79 | 3.87 | 76.6 |
| 3 | 17.38 | 5.71 | 99.2 |
| 2 | 13.7 | 6.05 | 82.7 |
| 0.5 | 4.9 | 6.05 | 29.5 |

### 3.3. Quantitative performance evaluation

Quantitative metrics are extracted from experimental measurements under STC (1000 W/m², 25 °C) to evaluate static accuracy and dynamic response. The results are summarized in Table 4.

Table 4. Summary of quantitative performance metrics

| Parameter | Measured value |
|---|---|
| Maximum power (MPP) | 99.2 W |
| MPP deviation | 0.8% |
| RMSE (normalized) | 0.015 |
| Settling time | 12 ms |
| Overshoot | < 1.5% |
| Voltage ripple | < 2% |
| Converter efficiency | 94% |

#### 3.3.1. Maximum power point deviation

The percentage deviation at the MPP is calculated as:

$$Error_{MPP}(\%) = \frac{|P_{meas} - P_{ref}|}{P_{ref}} x100\%$$

where $P_{meas}$ is the measured maximum power and $P_{ref}$ is the rated maximum power. The measured maximum power is 99.2 W at approximately 3 Ω load, compared to the 100 W reference value, yielding an MPP deviation of 0.8%. This confirms high static accuracy at the nominal operating point.

#### 3.3.2. Root mean square error

The current tracking performance is evaluated using the root mean square error (RMSE):

$$RMSE = \sqrt{\frac{1}{N}\sum_{i=1}^{N}(I_{meas,i} - I_{ref,i})^2}$$

where $I_{meas}$ and $I_{ref}$ denote measured and reference currents, respectively. The normalized RMSE across sampled operating points of the I–V curve is 0.015, indicating minimal deviation from the reference characteristic.

#### 3.3.3. Dynamic performance

Transient performance is evaluated under abrupt load transitions between 20 Ω and 3 Ω. The emulator exhibits: i) settling time ≈ 12 ms, ii) overshoot < 1.5%, and iii) output voltage ripple < 2%. The response is monotonic without sustained oscillation, confirming stable DEC-based regulation.

#### 3.3.4. Converter efficiency

Converter efficiency is calculated as

$$\eta = \frac{P_{out}}{P_{in}} x100\%$$

Measured efficiency near the MPP region reaches 94%, confirming effective power conversion with limited switching losses.

### 3.4. Discussion

Simulation and experimental results demonstrate consistent reproduction of the nonlinear I–V and P–V characteristics of the reference PV module under STC. The operating point shifts smoothly from the open-circuit region toward the short-circuit region as load resistance decreases, consistent with physical PV

behavior. The LUT-based reference model preserves the intrinsic power–voltage relationship, while the DEC algorithm ensures stable real-time duty-cycle regulation. Peak power is achieved near 3 Ω load, aligning with the rated 100 W module specification.

Experimental results closely match simulation trends despite implementation on a low-cost hardware platform consisting of an XL4016 buck converter and an Arduino Nano controller. The DEC regulator maintains monotonic convergence and prevents oscillatory behavior during load transitions. Boundary operating conditions are correctly reproduced: under no-load, the output converges to open-circuit voltage with negligible current; under heavy load, the emulator operates in the high-current region without instability or saturation. The agreement between simulation and hardware validation confirms that the proposed architecture reliably emulates realistic PV electrical characteristics for laboratory-scale converter evaluation.

## 4. CONCLUSION

A DEC-regulated buck-converter-based PV emulator has been designed and experimentally validated under standard test conditions (1000 W/m², 25 °C). The system achieves 0.8% MPP deviation, 0.015 normalized RMSE, 12 ms settling time, <1.5% overshoot, <2% output ripple, and 94% peak efficiency near the MPP region. The LUT-integrated control architecture enables accurate nonlinear PV characteristic reproduction with low computational complexity, making the proposed system suitable for controlled laboratory evaluation of PV-powered power electronic converters.

Validation is limited to standard test conditions with fixed irradiance and temperature. Dynamic environmental variations were not experimentally evaluated. The implementation is restricted to a single 100 W PV module model, and scalability to higher power levels or multi-module configurations requires further investigation. Future work will extend the emulator to variable irradiance scenarios and include comparative evaluation against conventional PID-based control under dynamic disturbances.

## FUNDING INFORMATION

The authors would like to express their sincere gratitude to the University of Lampung for the research support and laboratory facilities provided. This work was financially supported through the Gurubesar BLU Unila research grant scheme.

## AUTHOR CONTRIBUTIONS STATEMENT

This journal uses the Contributor Roles Taxonomy (CRediT) to recognize individual author contributions, reduce authorship disputes, and facilitate collaboration.

| Name of Author | C | M | So | Va | Fo | I | R | D | O | E | Vi | Su | P | Fu |
|---|---|---|---|---|---|---|---|---|---|---|---|---|---|---|
| Ahmad Saudi Samosir | ✓ | ✓ | ✓ | ✓ | ✓ | ✓ | | ✓ | ✓ | ✓ | | ✓ | | ✓ |
| Dikpride Despa | | ✓ | | | ✓ | ✓ | | | | ✓ | ✓ | ✓ | | |
| Herri Gusmedi | ✓ | | | ✓ | | ✓ | ✓ | | ✓ | ✓ | ✓ | | ✓ | ✓ |
| Sony Ferbangkara | | | ✓ | | ✓ | ✓ | ✓ | ✓ | | ✓ | | | ✓ | |

C : **C**onceptualization
M : **M**ethodology
So : **So**ftware
Va : **Va**lidation
Fo : **Fo**rmal analysis
I : **I**nvestigation
R : **R**esources
D : **D**ata Curation
O : Writing - **O**riginal Draft
E : Writing - Review & **E**diting
Vi : **Vi**sualization
Su : **Su**pervision
P : **P**roject administration
Fu : **Fu**nding acquisition

## CONFLICT OF INTEREST STATEMENT

Authors state no conflict of interest.

## DATA AVAILABILITY

The data that support the findings of this study, including the lookup table (LUT) reference data of the PV module, experimental measurement data under various resistive loading conditions, and dynamic response data of the proposed PV emulator, are available from the corresponding author, [ASS], upon reasonable request.

## REFERENCES


[1] W. C. Sinke, "Development of photovoltaic technologies for global impact," *Renewable Energy*, vol. 138, pp. 911–914, Aug. 2019, doi: 10.1016/j.renene.2019.02.030.

[2] V. Milenov, I. Bachev, L. Stoyanov, Z. Zarkov, and V. Lazarov, "Indoor testing of solar panels," in *2020 12th Electrical Engineering Faculty Conference (BulEF)*, Sep. 2020, pp. 1–4. doi: 10.1109/BulEF51036.2020.9326084.

[3] A. Al Mansur, M. I. Islam, M. A. ul Haq, M. H. Maruf, A. Shihavuddin, and M. R. Amin, "Investigation of PV modules electrical characteristics for laboratory experiments using halogen solar simulator," in *2020 2nd International Conference on Sustainable Technologies for Industry 4.0 (STI)*, Dec. 2020, pp. 1–6. doi: 10.1109/STI50764.2020.9350496.

[4] A. A. de M. Bento and R. P. Santiago, "A low cost photovoltaic panel emulator," in *2019 IEEE 15th Brazilian Power Electronics Conference and 5th IEEE Southern Power Electronics Conference (COBEP/SPEC)*, Dec. 2019, pp. 1–5. doi: 10.1109/COBEP/SPEC44138.2019.9065629.

[5] A. Boucharef, A. Tahri, F. Tahri, S. Silvestre, and M. Bourahla, "Solar module emulator based on a low-cost microcontroller," *Measurement*, vol. 187, p. 110275, Jan. 2022, doi: 10.1016/j.measurement.2021.110275.

[6] A. N. Ali, K. Premkumar, M. Vishnupriya, B. V. Manikandan, and T. Thamizhselvan, "Design and development of realistic PV emulator adaptable to the maximum power point tracking algorithm and battery charging controller," *Solar Energy*, vol. 220, pp. 473–490, May 2021, doi: 10.1016/j.solener.2021.03.077.

[7] C.-T. Ma, Z.-Y. Tsai, H.-H. Ku, and C.-L. Hsieh, "Design and implementation of a flexible photovoltaic emulator using a GaN-based synchronous buck converter," *Micromachines*, vol. 12, no. 12, p. 1587, Dec. 2021, doi: 10.3390/mi12121587.

[8] R. Ayop, C. W. Tan, S. N. Syed Nasir, K. Y. Lau, and C. Ling Toh, "Buck converter design for photovoltaic emulator application," in *2020 IEEE International Conference on Power and Energy (PECon)*, Dec. 2020, pp. 293–298. doi: 10.1109/PECon48942.2020.9314582.

[9] J. S. Z. Lee, R. H. G. Tan, N. M. L. Tan, and T. S. Babu, "Development Of PV Emulator For Partial Shading Condition With Processor-In-The-Loop Simulation Utilizing Real-Time Microcontoller," in *2023 IEEE Industrial Electronics and Applications Conference (IEACon)*, IEEE, Nov. 2023, pp. 116–121. doi: 10.1109/IEACon57683.2023.10370279.

[10] M. Alaoui, H. Maker, A. Mouhsen, and H. Hihi, "Real-time emulation of photovoltaic energy using adaptive state feedback control," *SN Applied Sciences*, vol. 2, no. 3, p. 492, Mar. 2020, doi: 10.1007/s42452-020-2294-2.

[11] A. Harrison, N. H. Alombah, S. Kamel, S. S. M. Ghoneim, I. El Myasse, and H. Kotb, "Towards a simple and efficient implementation of solar photovoltaic emulator: an explicit PV model based approach," in *The 4th International Electronic Conference on Applied Sciences*, Nov. 2023, p. 261. doi: 10.3390/ASEC2023-16268.

[12] I. Moussa and A. Khedher, "Photovoltaic emulator based on PV simulator RT implementation using XSG tools for an FPGA control: Theory and experimentation," *International Transactions on Electrical Energy Systems*, vol. 29, no. 8, 2019, doi: 10.1002/2050-7038.12024.

[13] H. A. Khawaldeh, M. Al-soeidat, D. D. Lu, and L. Li, "Simple and fast dynamic photovoltaic emulator based on a physical equivalent PV-cell model," *The Journal of Engineering*, vol. 2021, no. 5, pp. 276–285, May 2021, doi: 10.1049/tje2.12032.

[14] H. A. Khawaldeh, M. Al-Soeidat, M. Farhangi, D. D.-C. Lu, and L. Li, "Efficiency improvement scheme for PV emulator based on a physical equivalent PV-cell model," *IEEE Access*, vol. 9, pp. 83929–83939, 2021, doi: 10.1109/ACCESS.2021.3086498.

[15] I. D. G. Jayawardana, C. N. M. Ho, M. Pokharel, and G. E. Valderrama, "A fast-dynamic control scheme for a power-electronics-based PV emulator," *IEEE Journal of Photovoltaics*, vol. 11, no. 2, pp. 485–495, Mar. 2021, doi: 10.1109/JPHOTOV.2020.3041188.

[16] M. Troviano and G. G. Oggier, "Low-cost photovoltaic emulator with a high-dynamic response for small satellite applications," *International Journal of Energy for a Clean Environment*, vol. 25, no. 6, pp. 1–12, 2024, doi: 10.1615/InterJEnerCleanEnv.2024050320.

[17] A. Harrison and N. H. Alombah, "A new high-performance photovoltaic emulator suitable for simulating and validating maximum power point tracking controllers," *International Journal of Photoenergy*, vol. 2023, pp. 1–21, Apr. 2023, doi: 10.1155/2023/4225831.

[18] A. Harrison and N. H. Alombah, "A new piecewise segmentation based solar photovoltaic emulator using artificial neural networks and a nonlinear backstepping controller," *Applied Solar Energy*, vol. 59, no. 3, pp. 283–304, Jun. 2023, doi: 10.3103/S0003701X23600285.

[19] N. H. Alombah, A. Harrison, S. Kamel, H. B. Fotsin, and M. Aurangzeb, "Development of an efficient and rapid computational solar photovoltaic emulator utilizing an explicit PV model," *Solar Energy*, vol. 271, 2024, doi: 10.1016/j.solener.2024.112426.

[20] A. Harrison *et al.*, "Enhanced control strategy for photovoltaic emulator operating in continuously changing environmental conditions based on shift methodology," *Scientific Reports*, vol. 14, no. 1, p. 13406, Jun. 2024, doi: 10.1038/s41598-024-64092-7.

[21] W. Zhu *et al.*, "A novel simplified buck power system control algorithm: Application to the emulation of photovoltaic solar panels," *Computers and Electrical Engineering*, vol. 116, p. 109161, May 2024, doi: 10.1016/j.compeleceng.2024.109161.

[22] N. Tulasi, S. Divya, and N. Kumaresan, "A comprehensive design and analysis of solar PV emulator," *2025 IEEE North-East India International Energy Conversion Conference and Exhibition, NE-IECCE 2025*, 2025, doi: 10.1109/NE-IECCE64154.2025.11183052.

[23] Y. El asri *et al.*, "PV Emulator based on DC-DC buck converter and PI Controller," *EPJ Web of Conferences*, vol. 330, 2025, doi: 10.1051/epjconf/202533001002.

[24] A. S. Samosir, T. Sutikno, and L. Mardiyah, "Simple formula for designing the PID controller of a DC-DC buck converter," *International Journal of Power Electronics and Drive Systems (IJPEDS)*, vol. 14, no. 1, p. 327, Mar. 2023, doi: 10.11591/ijpeds.v14.i1.pp327-336.

[25] A. S. Samosir, S. R. Sulistiyanti, H. Gusmedi, and A. F. Huda, "Modeling and simulation of buck converter-based PV emulator," in *2023 International Conference on Converging Technology in Electrical and Information Engineering (ICCTEIE)*, Oct. 2023, pp. 27–31. doi: 10.1109/ICCTEIE60099.2023.10366746.

[26] A. S. Samosir, H. Gusmedi, and A. F. Huda, "Design and implementation of PV emulator based on synchronous buck converter using Arduino Nano microcontroller," *International Journal of Power Electronics and Drive Systems (IJPEDS)*, vol. 16, no. 1, p. 448, Mar. 2025, doi: 10.11591/ijpeds.v16.i1.pp448-456.

[27] A. S. Samosir and A. H. M. Yatim, "Implementation of dynamic evolution control of bidirectional DC-DC converter for interfacing ultracapacitor energy storage to fuel-cell system," *IEEE Transactions on Industrial Electronics*, vol. 57, no. 10, pp. 3468–3473, 2010, doi: 10.1109/TIE.2009.2039458.

[28] A. S. Samosir and A. H. M. Yatim, "Dynamic evolution control for synchronous buck DC-DC converter: Theory, model and simulation," *Simulation Modelling Practice and Theory*, vol. 18, no. 5, pp. 663–676, 2010, doi: 10.1016/j.simpat.2010.01.010.

[29] T. Nguyen-Duc, H. Nguyen-Duc, T. Le-Viet, and H. Takano, "Single-diode models of PV modules: a comparison of conventional approaches and proposal of a novel model," *Energies*, vol. 13, no. 6, p. 1296, Mar. 2020, doi: 10.3390/en13061296.

[30] J. M. Álvarez *et al.*, "Analytical modeling of current-voltage photovoltaic performance: an easy approach to solar panel behavior," *Applied Sciences*, vol. 11, no. 9, p. 4250, May 2021, doi: 10.3390/app11094250.

[31] J. Li, R. Li, Y. Jia, and Z. Zhang, "Prediction of I–V characteristic curve for photovoltaic modules based on convolutional neural network," *Sensors*, vol. 20, no. 7, p. 2119, Apr. 2020, doi: 10.3390/s20072119.
[32] C. Zhang, Y. Zhang, J. Su, T. Gu, and M. Yang, "Modeling and prediction of PV module performance under different operating conditions based on Power-Law I – V model," *IEEE Journal of Photovoltaics*, vol. 10, no. 6, pp. 1816–1827, Nov. 2020, doi: 10.1109/JPHOTOV.2020.3016607.
[33] D. Revati and E. Natarajan, "I-V and P-V characteristics analysis of a photovoltaic module by different methods using Matlab software," *Materials Today: Proceedings*, vol. 33, pp. 261–269, 2020, doi: 10.1016/j.matpr.2020.04.043.
[34] M. Seapan, Y. Hishikawa, M. Yoshita, and K. Okajima, "Temperature and irradiance dependences of the current and voltage at maximum power of crystalline silicon PV devices," *Solar Energy*, vol. 204, pp. 459–465, Jul. 2020, doi: 10.1016/j.solener.2020.05.019.
[35] T. N. Olayiwola, S.-H. Hyun, and S.-J. Choi, "Photovoltaic modeling: a comprehensive analysis of the I–V characteristic curve," *Sustainability*, vol. 16, no. 1, p. 432, Jan. 2024, doi: 10.3390/su16010432.

## BIOGRAPHIES OF AUTHORS

**Ahmad Saudi Samosir** is a lecturer in Electrical Engineering Department at the Universitas Lampung, Lampung, Indonesia. He received his B.Eng., M.Eng., and Ph.D. degrees in Electrical Engineering from Universitas Sumatera Utara, Institut Teknologi Bandung, and Universiti Teknologi Malaysia, in 1995, 1999, and 2010, respectively. He has been a Professor at Universitas Lampung Indonesia since 2017. He is currently a Dean of Postgraduate Faculty of Universitas Lampung. His research interests include power electronics design, controller and their applications in renewable energy, electric vehicles, and industrial applications. He can be contacted at email: ahmad.saudi@eng.unila.ac.id or saudi.ahmad@gmail.com.

**Dikpride Despa** is a lecturer in Electrical Engineering Department at Universitas Lampung, Lampung Indonesia. She received her Dr. Eng Degree in Electrical engineering from Kyushu Institute of Technology (KYUTECH) Japan, in 2012. She is currently a head of research and community service of Universitas Lampung. Her research interest includes power system monitoring, stability and control, energy audit, renewable energy, and instrumentation. She can be contacted at email: despa@eng.unila.ac.id.

**Herri Gusmedi** is a lecturer in Electrical Engineering Department at the Universitas Lampung, Lampung, Indonesia. He received his B.Eng., M.Eng. degree in Electrical Engineering from Universitas Sriwijaya and Institut Teknologi Bandung, respectively, in 1995, 2000. Served as head of Electric power system laboratory at Universitas Lampung, Indonesia, since 2020. His research interests include system reliability design, economical operation, power converter, and renewable energy, especially photovoltaic. He can be contacted at email: herri.gusmedi@eng.unila.ac.id.

**Sony Ferbangkara** is a lecturer in the Electrical Engineering Department at Universitas Lampung, Lampung, Indonesia. He received his B.Eng. degree in Electrical Engineering from Universitas Lampung in 2008. He completed his M.Eng. degree in Electrical Engineering at Universitas Lampung in 2022 and obtained his professional engineer (Ir.) qualification from Universitas Lampung in 2025. His research interests include programming and cyber-physical systems, with additional interests in computer networks and smart city technologies. He can be contacted at email: sony.ferbangkara@eng.unila.ac.id.